Implementation of integral viscoelastic constitutive models in OpenFOAM® computational library

Manuel Silvino Batalha de Araújo, Célio Fernandes, Luís Lima Ferrás, Željko Tukovic, Hrvoje Jasak, and João Miguel Nóbrega

Citation: AIP Conference Proceedings **1662**, 020005 (2015); doi: 10.1063/1.4918875
View online: http://dx.doi.org/10.1063/1.4918875
View Table of Contents: http://scitation.aip.org/content/aip/proceeding/aipcp/1662?ver=pdfcov
Published by the AIP Publishing

Implementation of Integral Viscoelastic Constitutive Models in OpenFOAM® Computational Library

Manuel Silvino Batalha de Araújo[1, b)], Célio Fernandes[2, c)], Luís Lima Ferrás[2, d)], Željko Tukovic[3, e)], Hrvoje Jasak[3, 4, f)] and João Miguel Nóbrega[2, a)]

[1]*Universidade Federal do Pará, Instituto de Ciências Exatas e Naturais, Faculdade de Matemática - 66075-110 - Belem, PA – Brasil*
[2]*Institute for Polymers and Composites/I3N, University of Minho, Campus of Azurém, 4800-058 Guimarães, Portugal*
[3]*Faculty of Mechanical Engineering and Naval Architecture, University of Zagreb, Croatia*
[4]*Wikki Ltd., London, United Kingdom*

[a)]Corresponding author: mnobrega@dep.uminho.pt
[b)]silvino@ufpa.br
[c)]cbpf@dep.uminho.pt
[d)]luis.ferras@dep.uminho.pt
[e)]zeljko.tukovic@fsb.hr
[f)]h.jasak@wikki.co.uk, hrvoje.jasak@fsb.hr

Abstract. This work reports the implementation and verification of a new solver in OpenFOAM® open source computational library, able to cope with integral viscoelastic models based on the integral upper-convected Maxwell model. The code is verified through the comparison of its predictions with analytical solutions and numerical results obtained with the differential upper-convected Maxwell model.

INTRODUCTION

From the early nineteen-nineties onwards, we have witnessed a great evolution in computer's performance. This progress promoted the creation and development of powerful computational codes for science, industry, pedagogical or even for entertainment purposes. Among these codes, with particular interest for the industry are the ones related to the modeling of highly complex systems, because nowadays, in a high competition framework, numerical modeling codes have a major role on design processes, assuring savings of substantial resources such as time, money and raw materials.

During the initial stages, numerical modelling tools were based either on proprietary or in-house codes. Due to the high cost of the former software licenses, and since the last group codes were not available for general use, the employment of numerical modeling was rather restricted to academic studies. As time passed by, open source numerical codes started being developed [1–5] but, at the beginning, their impact was very low, mainly due to the low confidence of potential users.

During the last decade, the computational modelling communities witnessed a major change in that paradigm, as the teams involved on their development were significantly enlarged and became better organized. As a direct outcome, nowadays, there are open source numerical codes as powerful as the major proprietary software. Additionally, due to the large number of persons involved in their development, covering a large range of research/industrial fields, the impact of some open source codes [4, 6] became extremely significant for science and industry, and their importance is growing on a daily basis.

Novel Trends in Rheology VI
AIP Conf. Proc. 1662, 020005-1–020005-8; doi: 10.1063/1.4918875

In this work we are interested on modelling the flow of fluids, for which there are several commercial and noncommercial modelling codes. These numerical codes have to solve a system of partial differential equations that govern the fluid behavior, encompassing at least the conservation of mass and momentum. For more complex fluids, a new set of equations (constitutive equations) are added to the system, relating the stress and velocity fields. There are a large number of constitutive equations, able to cope with the most simple, Newtonian, to the most complex, viscoelastic, behaviors [7,8], being the viscoelastic modeling an increasing area of research.

A large number of constitutive equations were developed for viscoelastic fluids, some empirical and other with strong physical foundations. The currently available macroscopic constitutive equations can be divided in two main types: differential and integral. Some of the constitutive equations, e.g. Maxwell [7] are available both in differential and integral types. However, relevant integral models, like K-BKZ [9,10], just possesses the integral form.

Integral constitutive equations are difficult to handle numerically, because a large amount of information must be stored, in order to keep track of the material deformation in a Lagrangian sense [11, 12]. As a consequence, one can find a large number of works dealing with differential viscoelastic constitutive models [13-17], using different discretization methods using an Eulerian approach, the most natural framework for differential models. Regarding integral constitutive equations, the contributions are scarcer. Most of them employ a Lagrangian approach that comprises additional computational difficulties, related to the manipulation of a large amount of data and dynamic/moving meshes [11, 12]. The formulation based on the deformation fields, proposed by Peters et al. [18] and subsequently improved by Hulsen et al. [19], allowed the implementation of integral viscoelastic models in an Eulerian framework [20], thus facilitating the use of these models.

The main objective of this work is to implement integral viscoelastic model in an open source numerical code. From the fluid flow open source codes available, OpenFOAM® (Open source Fluid Operation And Manipulation) computational library is one of the most preeminent. This open source code is being developed simultaneously by a large number of groups around the world [21], and, it already comprises several solvers able to deal with differential constitutive viscoelastic models, using an Eulerian approach [17, 22].

Although very good results can be obtained with these solvers, integral models are not yet implemented, therefore, in this work we describe the implementation of a new solver in OpenFOAM® able to deal with integral constitutive models [20, 23], based on the upper-convected Maxwell (UCM) model.

The manuscript is organized as follows. The next section contains a general description of the governing equations, and is followed by the description of the discretization methodology adopted. The numerical implementation is then verified for the UCM Model through the comparison of the code predictions with analytical results, for a simple problem, and with the results obtained with the same constitutive model following the differential viscoelastic model, for more complex case studies.

GOVERNING EQUATIONS

The governing equations for confined flow of incompressible fluids are the continuity,

$$\nabla \cdot \mathbf{u} = 0 \tag{1}$$

and the momentum,

$$\rho \frac{\partial \mathbf{u}}{\partial t} + \rho \nabla \cdot (\mathbf{u}\mathbf{u}) = -\nabla p + \nabla \cdot \boldsymbol{\tau} + \rho g \tag{2}$$

equations, where $\mathbf{u}$ is the velocity vector, p is the pressure, ρ is the fluid density, g is the gravitational acceleration and $\boldsymbol{\tau}$ is the deviatoric stress tensor. In order to obtain a closed system of equations, a constitutive equation for $\boldsymbol{\tau}$ must be provided, and, for this work, we have chosen the a generalized integral model,

$$\boldsymbol{\tau}(t) = \int_{-\infty}^{t} M(t-t')f\left(\mathbf{B}_{t'}(x,t)\right)dt' \tag{3}$$

where $M(t-t') = \frac{a}{\lambda} e^{-\frac{(t-t')}{\lambda}}$ is the memory function, t and t' represent the current and the elapsed time, respectively, a, λ are model parameters, $\mathbf{B}_{\mathrm{i}}(x,t)$ is the Finger strain tensor, a field that measures the deformation of the fluid element at position x, and $f(\mathbf{B}_{\mathrm{i}}(x,t))$ is a function of the Finger tensor, being given by $f(\mathbf{B}_{\mathrm{i}}(x,t)) = H(I_1, I_2)\mathbf{B}_{\mathrm{i}}(x,t)$. The function $H(I_1, I_2)$ is 1 for the UCM model, and, it is given by

$$H(I_1, I_2) = \frac{\alpha}{\alpha + \beta I_1 + (1-\beta) I_2} \quad (4)$$

for the K-BKZ model, where I_1 and I_2 stand for the first and second invariants of the Finger tensor and α and β are model parameters.

NUMERICAL METHOD

On the implemented solver the system of Eqs. 1, 2 and 3 is solved using a methodology based on the finite volume method. The PISO (Pressure Implicit with Splitting of Operators) method was used to couple velocity, pressure and stress fields (although it was originally developed to deal with Newtonian fluids [24]). For the numerical solution of the velocity and stress discretized linear systems of equations we used the biconjugate gradient stabilized method, while for the pressure, the conjugate gradient method was used.

The discretization schemes used are central differences for the diffusive terms and upwind for the convective terms.

Evaluation of the Stress Tensor

To evaluate the extra-stress tensor we employ the deformation fields method introduced by Peters et al. [18] and subsequently improved by Hulsen et al. [19], using a methodology proposed by Tomé et al. [20] for the finite difference method, that was here adapted to the finite volume method framework.

To evaluate Eq. 3, two major steps are required: (1) define an approximation for the integral and, (2) devise an equation for the evolution in time of the Finger tensor. Although these steps have already been described elsewhere [18, 23] for ease of understanding, they are now briefly described.

First, the time interval]–∞,t] is divided into a finite number of $N-1$ subintervals $\left]-\infty, t_0^{'}\right]$, $\left]t_0^{'}, t_1^{'}\right]$,…, $\left]t_{N-1}^{'}, t_N^{'} = t\right]$, so that the integral of Eq. 3 can be rewritten as:

$$\boldsymbol{\tau}(t) = \int_{-\infty}^{0} M(t-t^{'}) f\left(\mathbf{B}_{t^{'}}(x,t)\right) dt^{'} + \sum_{k=0}^{k_{\max}} \int_{t_k^{'}}^{t_{k+2}^{'}} M(t-t^{'}) f\left(\mathbf{B}_{t^{'}}(x,t)\right) dt^{'} \quad (5)$$

Note that for $t' < 0$ we assume that $\mathbf{B}_i(x,t) = \mathbf{B}_{i0}(x,t)$.

For the evaluation of the first integral on the right-hand-side (rhs) of Eq. 5, a simple integration is performed, since the exact value can be easily obtained ($f(\mathbf{B}(t, t')$ is constant). To approximate the second integral on the rhs of Eq. 5 a second order integration formula is employed.

For the evolution and convection of the Finger tensor along time and space, we used the transport equation proposed by Peters et al. [18],

$$\frac{\partial \mathbf{B}_{t^{'}}(x,t)}{\partial t} + \nabla \cdot \left(\mathbf{u}\mathbf{B}_{t^{'}}(x,t)\right) - \left((\nabla \mathbf{u})^T \cdot \mathbf{B}_{t^{'}}(x,t) + \mathbf{B}_{t^{'}}(x,t) \cdot \nabla \mathbf{u}\right) = 0 \quad (6)$$

This equation was solved with the finite volume method, with the numerical schemes described before. Note that, when numerically solving the equation, the time t' is kept constant for each Finger tensor, since t' is a label for the moment of creation of the tensor [18].

SOLVER VERIFICATION

Case Study 1

In order to assess and validate the code implementation, initially we compared the numerical results with the analytical solution for the start-up Couette flow of an UCM viscoelastic fluid, as depicted in Fig. 1, assuming a known velocity field.

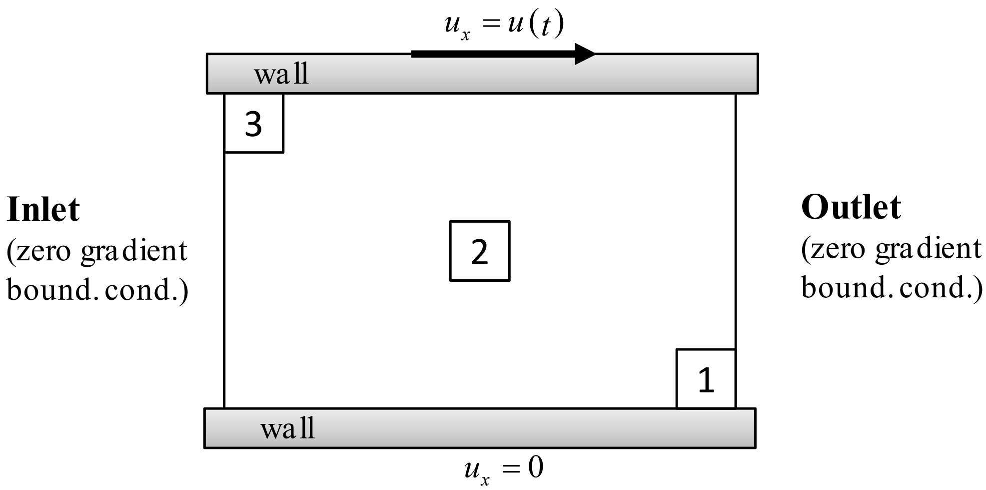

FIGURE 1. Schematic of the start-up Couette flow used in the numerical simulations.

A velocity field is imposed through all the domain, using the following equation

$$u_x = \begin{cases} 0 & ,t < 0 \\ \dot{\gamma} y & ,t \geq 0 \end{cases} \quad ,u_y = 0 \tag{7}$$

and, from the moment $t = 0$ onwards, we measure the evolution of the stress fields. Note that in the moment right before $t = 0$ the fluid is at rest, and therefore, the stress field is assumed to be null.

For this problem, there is an analytical solution for the evolution of the stress components that is given by,

$$\tau_{xx} = 2a\dot{\gamma}^2\lambda^2\left(1-\exp\left(-\frac{t}{\lambda}\right)\left(1+\frac{t}{\lambda}\right)\right),\ \tau_{xy} = a\lambda\dot{\gamma}\left(1-\exp\left(-\frac{t}{\lambda}\right)\right),\ \tau_{yy} = 0 \tag{6}$$

where $\dot{\gamma}$ is the shear rate [23].

In the numerical simulations the stress growth along time was monitored at three specific points of the geometry, identified in Fig. 1. The mesh used in the simulations is composed of 20 cells along the thickness and 50 deformation fields.

In Fig. 2 we can see the evolution in time of τ_{xx} and τ_{yy} (at position 2). As desired, there is a very good agreement between the analytical and the numerical results. The results are equal for the other two monitored points.

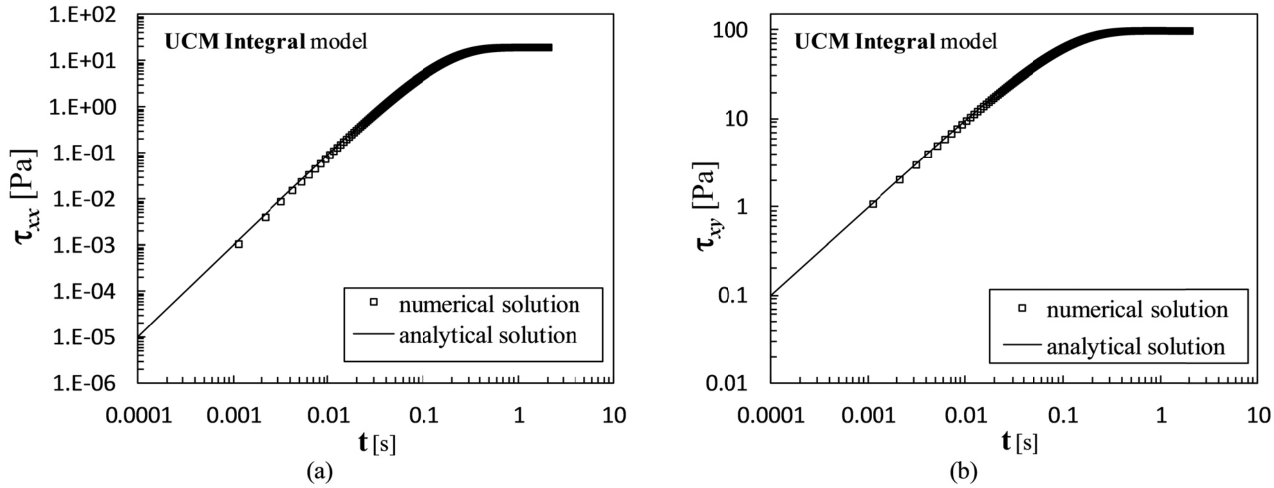

FIGURE 2. Growth of the normal, τ_{xx}, and shear, τ_{xy}, stresses, of the integral UCM model. Comparison between numerical and analytical solutions.

After a certain period, the stresses tend to the steady state solution, as expected, since the imposed velocity profile remains constant along time.

Case Study 2

A second case study was used to further reinforce the robustness of the new numerical implementation. For this case, the following velocity profile was imposed at the top wall of the Couette simulation (Fig. 1),

$$u_x = \begin{cases} v_0 \dfrac{t}{t_c} & ,0 \le t < t_c \\ v_0 & ,t \ge t_c \end{cases} \quad ,u_y = 0\,, \tag{6}$$

where v_0 was set to 0.001 m.s^{-1}, and $t_c = 1.5$s. The numerical solution obtained with the implemented integral UCM model, was now compared with the numerical results provided by the differential UCM model, which is available in OpenFOAM® [17]. The computed results are illustrated in Fig. 3, for the two most relevant components of the stress tensor. Again, an excellent agreement was observed, between the two different formulations.

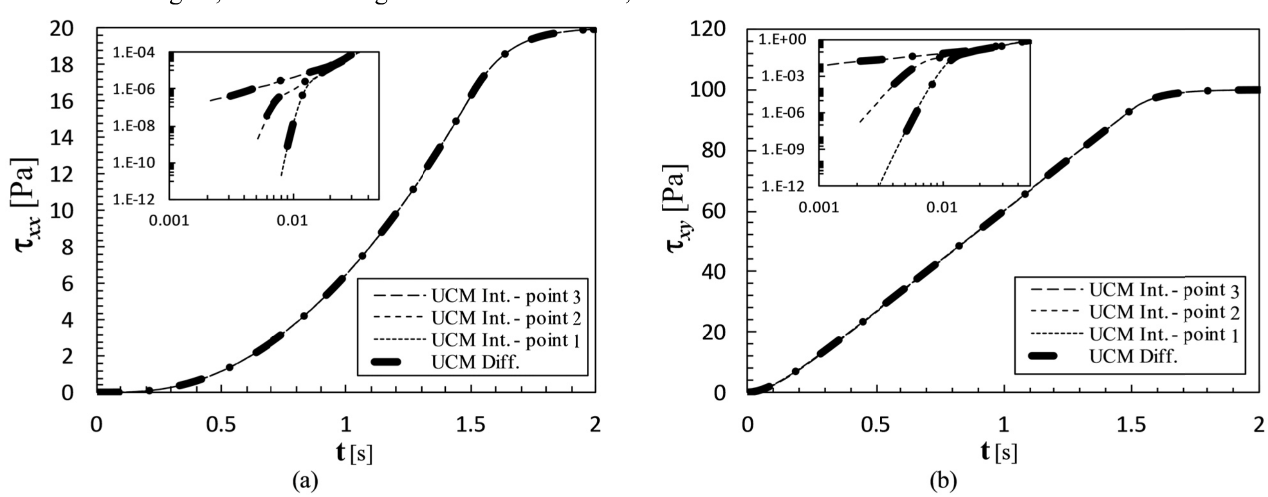

FIGURE 3. Growth of the normal, τ_{xx}, and shear, τ_{xy}, stresses, for the integral UCM model. Comparison between the integral and the differential viscoelastic model predictions.

Case study 3

A third case study was also included in this work, by comparing the velocity and stress profiles, obtained for the Poiseuille flow (Fig. 4) of the differential and integral UCM models.

The numerical simulations were performed in the geometry and with the boundary conditions shown in Fig. 4. The problem is transient, and, a constant velocity profile (U = 0.001 m.s^{-1}) is imposed at the inlet, while a null velocity field was imposed in the rest of the flow channel. The velocity and stress profiles were extracted at the center of the channel (x = 15H).

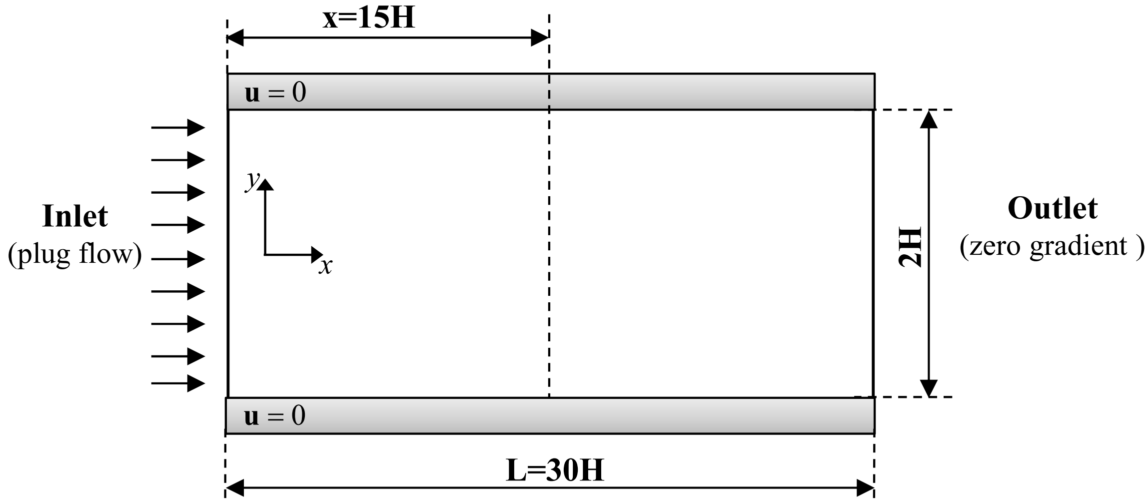

FIGURE 4. Schematic of the Poiseuille flow used in the numerical simulations.

Fig. 5 shows the different velocity profiles at for four different instants of time, for both differential and integral UCM models. Similarly to the previous case studies, an almost exact match was obtained, proving once again the accuracy of the new implemented solver.

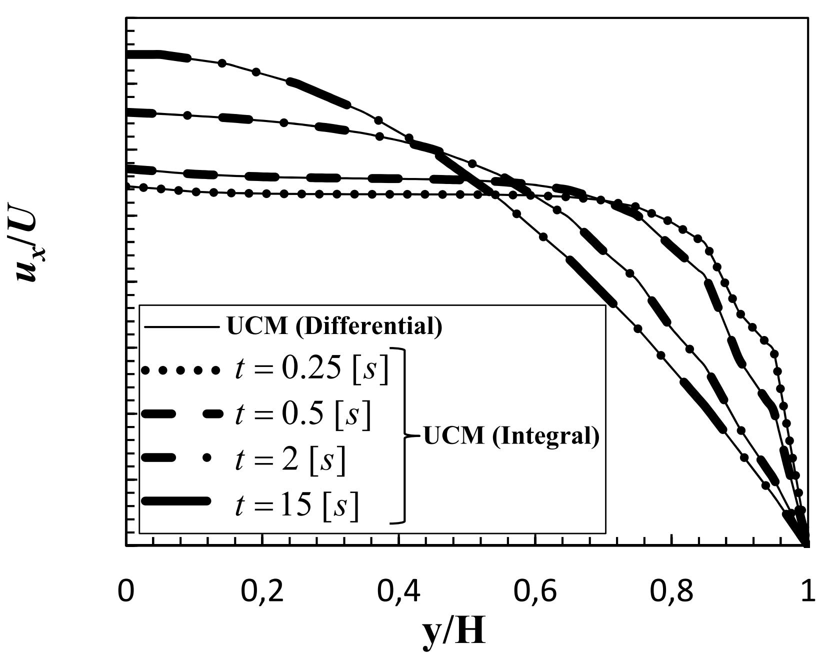

FIGURE 5. Profiles of the streamwise velocity component, u_x, for the Poiseuille flow at different instants and constant x = 15H.

As expected, the velocity profile evolves from a plug flow, due to the influence of the initial velocity field, to a parabolic profile, with the maximum velocity reaching the well know value of $1.5U$.

The evolution along time of the normal (τ_{xx}) and shear (τ_{xy}) stress components was also analyzed for this third case study (Figs. 6a and b). In this case one can notice a small deviation between the integral an differential formulations for the normal stress component at the initial time steps, however, as time advances, when the fully developed profiles are achieved, a perfect match between both models is found.

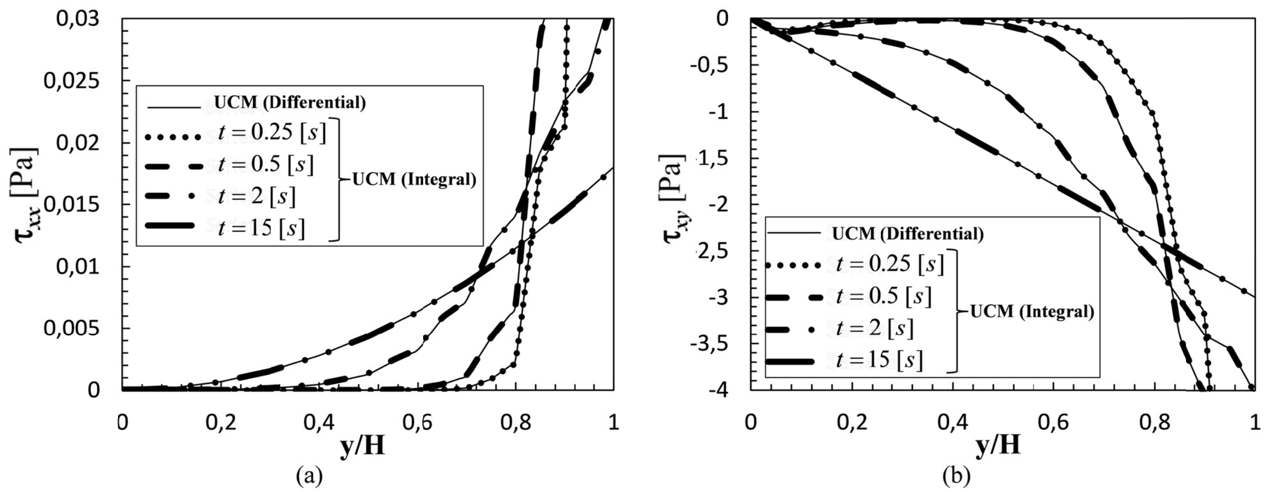

FIGURE 6. Profiles of the normal, τ_{xx}, and shear, τ_{xy}, stresses, for the integral UCM model. Comparison between the integral and the differential viscoelastic model predictions for the Poiseuille flow for different instants and constant $x = 15H$.

CONCLUSIONS

This work reports the implementation and verification of the integral upper-convected Maxwell viscoelastic model in OpenFOAM® computational library. The numerical implementation was verified with three case studies: the evolution of stress in a homogenous Couette flow and startup Couette and Poiseuille flows. The results predicted by the developed solver matches very well the analytical solution, for the first case study, and the results provided by a differential upper-convected Maxwell solver, for the last two. These comparisons proved the robustness and accuracy of the numerical implementation.

ACKNOWLEDGMENTS

M.S.B. de Araújo acknowledges funding from CAPES (Coordenação de Aperfeiçoamento de Pessoal de Nível Superior) – proc. BEX 1902-14-8. J.M. Nóbrega and L.L. Ferrás gratefully acknowledge funding from Fundação para a Ciência e Tecnologia (FCT) under the projects PEst-C/CTM/LA0025/2013 (Strategic Project - LA 25 - 2013-2014), project PTDC/MAT/121185/2010 and FEDER, via FCT.

REFERENCES

1 S. Plimpton, J. Comput. Phys. **117**, 1-19 (1995).
2 S. Popinet, J. Comput. Phys. **190**, 572–600 (2003).
3 B. J. Araújo, J. C. F. Teixeira, A. M. Cunha and C. P. T. Groth, Int. J. Numer. Methods Fluids. **59**, 801–815 (2009).
4 F. Palacios, J. Alonso, K. Duraisamy, M. Colonno, J. Hicken, A. Aranake, et al., “An open-source integrated computational environment for multi-physics simulation and design,” in: *51st AIAA Aerosp. Sci. Meet.* (Stanford University Unstructured (SU2), doi:10.2514/6.2013-287, 2013), pp. 1–60.

5 H. Jasak, H. G. Weller and N. Nordin, In-cylinder CFD simulation using a C++ object-oriented toolkit, SAE Technical Paper, (2004). doi:10.4271/2004-01-0110.
6 H. Jasak, A. Jemcov and Z. Tukovic, OpenFOAM®: A C ++ Library for Complex Physics Simulations, International Workshop on Coupled Methods in Numerical Dynamics 1–20 (2007).
7 R. B. Bird, R. C. Armstrong and O. Hassager, *Dynamics of polymeric liquids. Vol. 1: Fluid mechanics*, (A Wiley-Interscience Publication, John Wiley & Sons, 1987).
8 F. A. Morrison, *Understanding Rheology*, (Oxford University Press, 2001).
9 E. Mitsoulis, ISRN Polym. Sci. **2013**, 1–22 (2013).
10 B. Bernstein, E. A. Kearsley and L. J. Zapas, J. Rheol. **7**, 391-410 (1963).
11 F. M. Schmidt, J. F. Agassant, M. Bellet, L. Desoutter, J. Non-Newtonian Fluid Mech. **64**, 19–42 (1996).
12 R. Keunings, "Finite element methods for integral viscoelastic fluids". in Rheology Reviews 2003, edited by D. M. Binding and K. Walters (British Society of Rheology, 2003), pp. 167–195;
13 L. L. Ferrás, A. M. Afonso, M. A. Alves, J. M. Nóbrega, O. S. Carneiro and F. T. Pinho, J. Non-Newtonian Fluid Mech. **214**, 28-37 (2014).
14 M. A. Alves, F. T. Pinho and P. J. Oliveira, J. Non-Newtonian Fluid Mech. **97**, 207–232 (2001).
15 M. Zatloukal, J. Non-Newtonian Fluid Mech. **113**, 209–227 (2003).
16 M. F. Tomé, N. Mangiavacchi, J. A. Cuminato, A. Castelo, S. McKee, J. Non-Newtonian Fluid Mech. **106**, 61–106 (2002).
17 J. L. Favero, A. R. Secchi, N. S. M. Cardozo and H. Jasak, Comput. Aided Chem. **27**, 915–920 (2009).
18 E. A. J. F. Peters, M. A. Hulsen and B. H. A. A. van den Brule, J. Non-Newtonian Fluid Mech. **89**, 209–228 (2000).
19 M. A. Hulsen, E. A. J. F. Peters and B. H. A. A. van den Brule, J. Non-Newtonian Fluid Mech. **98**, 201–221 (2001).
20 M. F. Tomé, M. S. B. de Araujo, M. a. Alves and F. T. Pinho, J. Comput. Phys. **227**, 4207–4243 (2008).
21 http://www.openfoamworkshop.org.
22 F. Habla, H. Marschall, O. Hinrichsen, L. Dietsche, H. Jasak and J. L. Favero, Chem. Eng. Sci. **66**, 5487–5496 (2011).
23 M. S. Araújo, "Extensão de GENSMAC para escoamentos de fluidos governados pelos modelos integrais Maxwell e K-BKZ," Ph.D. thesis, USP São Carlos, 2006.
24 R. I. Issa, J. Comp. Phys. **62**, 40–65 (1986).